Original Paper

Estimating Antigen Test Sensitivity via Target Distribution Balancing: Development and Validation Study

Miguel Bosch^{1,2}, PhD; Adriana Moreno², MSc; Raul Colmenares², MSc; Jose Arocha¹, MSc; Sina Hoche¹, PhD; Auris Garcia¹, BSc; Daniela Hall¹, PhD; Dawlyn Garcia¹, MSc; Lindsey Rudtner¹, BSc; Nol Salcedo¹, MSc; Irene Bosch¹, PhD

Corresponding Author:

Irene Bosch, PhD IDX20 Inc 166 Clinton Road Brookline, MA United States

Phone: 1 6177347745 Email: ibosch@idx20.us

Abstract

Background: Sensitivity—expressed as percent positive agreement (PPA) with a reference assay—is a primary metric for evaluating lateral-flow antigen tests (ATs), typically benchmarked against a quantitative reverse transcription polymerase chain reaction (qRT-PCR). In SARS-CoV-2 diagnostics, ATs detect nucleocapsid protein, whereas qRT-PCR detects viral RNA copy numbers. Since observed PPA depends on the underlying viral load distribution (proxied by the number of cycle thresholds [Cts], which is inversely related to load), study-specific sampling can bias sensitivity estimates. Cohort differences—such as enrichment for high- or low-Ct specimens—therefore complicate cross-test comparisons, and real-world datasets often deviate from regulatory guidance to sample across the full concentration range. Although logistic models relating test positivity to Ct are well described, they are seldom used to reweight results to a standardized reference viral load distribution. As a result, reported sensitivities remain difficult to compare across studies, limiting both accuracy and generalizability.

Objective: The aim of this study was to develop and validate a statistical methodology that estimates the sensitivity of ATs by recalibrating clinical performance data—originally obtained from uncontrolled viral load distributions—against a standardized reference distribution of target concentrations, thereby enabling more accurate and comparable assessments of diagnostic test performance.

Methods: AT sensitivity is estimated by modeling the PPA as a function of qRT-PCR Ct values (PPA function) using logistic regression on paired test results. Raw sensitivity is the proportion of AT positives among PCR-positive samples. Adjusted sensitivity is calculated by applying the PPA function to a reference Ct distribution, correcting for viral load variability. This enables standardized comparisons across tests. The method was validated using clinical data from a community study in Chelsea, Massachusetts, demonstrating its effectiveness in reducing sampling bias.

Results: Over a 2-year period, paired ATs and qRT-PCR-positive samples were collected from 4 suppliers: A (n=211), B (n=156), C (n=85), and D (n=43). Ct value distributions varied substantially, with suppliers A and D showing lower Ct (high viral load) values in the samples, and supplier C skewed toward higher Ct values (low viral load). These differences led to inconsistent raw sensitivity estimates. To correct for this, we used logistic regression to model the PPA as a function of Cts and applied these models to a standardized reference Ct distribution. This adjustment reduced bias and enabled more accurate comparisons of test performance across suppliers.

Conclusions: We present a distribution-aware framework that models PPA as a logistic function of Ct and reweights results to a standardized reference Ct distribution to produce bias-corrected sensitivity estimates. This yields fairer, more consistent comparisons across AT suppliers and studies, strengthens quality control, and supports regulatory review. Collectively, our results provide a robust basis for recalibrating reported sensitivities and underscore the importance of distribution-aware evaluation in diagnostic test assessment.

¹IDX20 Inc, Brookline, MA, United States

²Info Analytics Innovations LLC, Houston, TX, United States

Trial Registration: ClinicalTrials.gov NCT05884515; https://clinicaltrials.gov/study/NCT05884515

JMIR Bioinform Biotech2025;6:e68476; doi: 10.2196/68476

Keywords: antigen test; COVID-19; positive percent agreement; real-world data; sensitivity estimation; PPA

Introduction

Antigen tests (ATs) have been a common tool utilized to provide evidence for diagnosis and health care decisions and have been used as such for several decades [1-4]. During the COVID-19 pandemic, the worldwide use of ATs demonstrated relevance for disease monitoring and diagnosis of new cases [5,6]. ATs are rapid, economical, and portable; can be self-administered; are quick to develop; and provide direct evidence for the presence of the pathogen in the tested sample—this combination is not equaled by more sophisticated laboratory tests. Due to its increasing use, it is important to accurately evaluate the AT performance for quality and regulatory control.

The common statistic used to evaluate the positive agreement performance of ATs has been sensitivity, calculated over a set of samples known to be positive by a gold standard reference. However, the sensitivity of ATs is known to be strongly dependent on the sample viral load [7-9]. Hence, the sensitivity per se is not an appropriate measure of the AT positive agreement performance because it is largely dependent on the distribution of the viral load of statistical support (ie, the set of samples used to calculate the statistic). Instead, a description of the percent positive agreement (PPA) as a function of viral load is a more accurate measure of positive agreement performance. The PPA function (PPAf) is commonly calculated with a logistic regression of the binary test result on positive agreement (1=agreement, 0=disagreement) against a variable related to the viral load. In the case of COVID-19, the viral load is commonly measured with the quantitative reverse transcription polymerase chain reaction (qRT-PCR) cycle threshold (Ct) result [10,11]; hence, the PPA is a function of the Cts.

Once the PPAf of a given AT supplier's product has been estimated from collected data in real-world application conditions, it is straightforward to estimate the expected sensitivity for any given Ct distribution or Ct sample set. This is particularly useful for equalizing the expected sensitivity to a common standard or reference distribution of Cts for a comparison of the performance across suppliers for product quality or regulatory purposes. This process removes the bias introduced into sensitivity by the circumstantial uneven representation of viral load in the statistical support (ie, the data used to calculate the statistic).

Common methods used to calculate the sensitivity of an AT product, whether for regulatory compliance or clinical diagnostic research purposes, typically involve collecting real-world test results paired with the qRT-PCR gold standard. However, in the case of lateral-flow ATs, sensitivity uncertainty does not adhere to a straightforward Bernoulli process, as the underlying positive agreement probability is not constant and is instead conditioned by viral load. To

accurately calculate sensitivity, it would be necessary to segment the collected samples based on the most influential variable affecting underlying probability, using a standard reference histogram. In our case, the influential variable is the viral load, measured as Cts. Yet, implementing such a process in the field with real-world data would be cumbersome and would require a much larger dataset. The proposed balancing method overcomes this challenge by adjusting the raw sensitivity calculation to any desired standardized reference distribution of the viral load, without the need for extended data collection and segmentation.

Methods

Study Description

We conducted a study of AT use in real-world conditions in the city of Chelsea, Massachusetts, during the years 2022-2023. The objectives of the study were multifold: (1) performing frequent COVID-19 testing at 2 vulnerable population sites (elderly housing), (2) evaluating the performance of ATs from different suppliers in the laboratory and in the real-world context, (3) collecting longitudinal (time series) AT data for qRT-PCR positive samples, and (4) implementing a digital AT data collection platform.

The participants of the study were enrolled after consent. The participant was provided with a single self-testing AT of any of the available 4 participating suppliers. The tests were home tests, and data were self-logged by the participants into an internet-based informatics platform. The participants registered the AT results (their own assessment) and uploaded a photograph of the test after completion (15 min). The fraction of positive AT tests was followed daily with paired qRT-PCR testing. A random number of negative ATs were also analyzed by PCR.

Support personnel were available on scheduled days throughout the week within the community to provide devices, training, and participant follow-up. This minimized potential confounding factors related to test interpretation and self-reporting via the app. In addition to textual reports, participants uploaded an image of their test result, allowing our team to perform retrospective verification. Discrepancies between self-reported results and staff-reviewed interpretations were found to be negligible, occurring in 5 eye assessments of 500 positive tests.

The data analyzed come from ATs provided by 4 different suppliers, labeled A through D, and the corresponding qRT-PCR test results, all of which were processed at a Clinical Laboratory Improvement Amendments—certified laboratory using the same RNA extraction as well as PCR protocol. The total negative qRT-PCR tests were 57 for A, 91 for B, 145 for C, and 114 for D, and positive

qRT-PCR tests were 211 for A, 156 for B, 84 for C, and 43 for D. Each participant was tested with a single brand (ie, AT supplier), so the distribution of viral load could be different between the data collected for each brand. These data were used to calculate AT performance statistics and demonstrate the methodology for distribution-balanced sensitivity according to a reference standard distribution. Lineage annotations used in this study for laboratory assays were Delta comparator (B.1.617.2/AY sublineages) using the US WA 1/1 isolate and Omicron (BA.5). Among Chelsea study participants in 2022-2023, we detected BA.1.1, BA.2, BA.2.12.1, BA.5, BA.5.1, BA.5.2, BA.5.2.1, BQ.1.1, BQ.1.1.4, BQ.1.1.5, BQ.1.1.4, and XBB.1.5. Clinical sample sequences were generated at the Broad Institute.

Ethical Considerations

This study was reviewed and approved by the Advarra Institutional Review Board (IRB) for protocol "Center of Complex Interventions – IDx20-001, Community frequent antigen testing to monitor COVID-19 in senior public housing setup" (Pro00059157). The most recent continuing review approval was granted on November 13, 2023, with approval through November 13, 2024. Advarra is registered with the Office for Human Research Protections/Food and Drug Administration (IRB #00000971) and conducts reviews in accordance with US HHS 45 CFR 46 and FDA 21 CFR 50/56. All procedures adhered to institutional and national ethical standards and the World Medical Association Declaration of Helsinki. In accordance with JMIR Publications requirements, the IRB review outcome is explicitly reported here.

Before any study procedures, participants were informed of the study purpose, procedures, potential risks and benefits, data uses, and their right to withdraw without penalty. Written informed consent was obtained from each participant using IRB-approved consent materials. No monetary compensation was given to participants. All study personnel completed human-subjects protection training prior to participant interaction.

Data were collected and stored under IRB-approved procedures to protect privacy and confidentiality. Only deidentified or aggregated data are presented in this study; no identifiable personal information is reported.

Any protocol amendments, consent-form changes, or reportable events (eg, unanticipated problems; adverse device effects; or protocol deviations that could affect participant rights, safety, or data integrity) were submitted to Advarra in accordance with IRB requirements before implementation.

PPA Function

As commonly used, AT operative reading involves steps of device reaction to the nasal swab sample, a waiting time after the sample is deposited, an observation using the naked eye, and interpretation of the results by the user. For all kits utilized (eg, cassettes), the user observed the presence or absence of a colored line in a test area (*test band*) on

a nitrocellulose strip of the lateral-flow test. The result is considered *positive* when the test band visualized (a color band) and can be distinguished from the no color or white background even if the color signal is faint, while a *negative* result is when the test band cannot be visualized by the user. For performance statistics, the result of the AT provided to the user is compared to the gold standard reference test [12], a COVID-19 qRT-PCR test conducted in a state-approved clinical laboratory.

For the positive agreement analysis of each AT supplier dataset, we compare only the AT results that have a paired positive qRT-PCR result (ie, having a positive qRT-PCR result in a parallel swab sample taken the same day and time as the AT swab sample). For the logistic regression analysis, we identified the AT results with a binary variable: 1 for a positive result (agreement with the standard test) and 0 for a negative result (disagreement with the standard test). The outcome of the user assessment can be described by a binary random variable. We modeled the PPAf with a logistic function, having the qRT-PCR Ct as the function domain (ie, the independent variable). Logistic regression is a well-known analysis to estimate the probability as a function of a dependent variable [13]. It has been used to describe the probability of positive agreement in ATs [14].

In addition to estimating the PPAf that characterized each AT supplier, the regression also accounts for the uncertainties of the probability function and parameters. We implement the logistic regression with a Bayesian approach, combining the objectives of (1) fitting the binary observed data and (2) honoring the Clopper-Pearson binomial confidence limits at the raw Ct data sensitivity prediction. Hence, the posterior model uncertainty description ensures compliance with the Clopper-Pearson confidence limits for the sensitivity at the raw Ct data. The numerical calculations are performed by Markov chain Monte Carlo methods.

The logistic model is a well-established method for modeling binary outcomes in which the probability, p(x), varies with a predictor variable, x, particularly when the probability increases monotonically with x. It assumes that the log-odds of the outcome (ie, the logit transformation of the probability) is a linear function of the predictor. Compared to the traditional approach to raw sensitivity estimation-which treats test outcomes as the result of a Bernoulli process with constant (homogeneous) probability-the logistic model offers a first-order improvement by accounting for the dependence of the outcome probability on the target concentration. Although alternative parametric models could be used to describe the relationship between probability and the predictor (eg, probit, splines), the logistic model provides a widely accepted and practical framework for improving sensitivity estimation accuracy. Logistic and probit models both yield nearly identical monotone dose-response curves; we selected the logistic model for its interpretability in terms of log-odds, its ability to directly estimate the concentration at which PPA=0.5, and its widespread use in diagnostics. Spline approaches are not appropriate in this context, as they do not satisfy the boundary

conditions of approaching 0 at the lower end and 1 at the upper end of the concentration axis.

Distribution-Balanced Sensitivity Method

The sensitivity, s, is the fraction of the positive agreement cases divided by the total positive cases in the experimental gold standard results (eg, collected real-world AT binary data on positive qRT-PCR cases). Based on the PPAf characterized for each AT supplier data, we can estimate the sensitivity for any set of Ct cases. Let us consider that the experimental data for a given AT supplier involves N cases with qRT-PCR cycle counts, $x = \{x_1, x_2, ...x_n, ..., x_N\}$. The expected value of the sensitivity is the average of the PPAf, p(x), over the cases:

$$E(s) = \frac{1}{N} \sum_{1}^{N} p(x_n)$$
 (1)

Likewise, the expected sensitivity over a data support with any Ct probability density function (PDF), g(x), is given by the probability product integration:

$$E(s) = \frac{1}{xf - x0} \int_{x0}^{xf} p(x)g(x)dx$$
 (2)

Equations 1 and 2 use the PPAf to calculate the expected sensitivity over a specific Ct data or distribution. Adequate comparison of sensitivity across different AT datasets

requires a transformation of raw sensitivity (ie, calculated from the observed data) to the expected sensitivity over a common reference of Ct data values, or a Ct support distribution (ie, histogram or PDF). Considering observed binary data for several AT suppliers, our proposed process to equalize the sensitivity support involves (1) estimating the PPAfs by logistic regression of the observed AT binary data for each one of the supplier's datasets; (2) defining a common reference Ct distribution by a PDF, g(x); and (3) calculating for each AT supplier dataset the estimated sensitivity over the common reference Ct support by equation (2).

Equation 2 can be evaluated by discretizing the Ct domain. Alternatively, it can be computed by Monte Carlo integration, drawing Ct realizations from the target distribution and applying equation 1 to each draw. To balance viral load distributions across assays, we select a reference Ct sample set as the empirical Ct distribution from supplier A and evaluate all other suppliers over this common range. The procedure is as follows: (1) for each nonreference supplier, fit a logistic regression for PPA as a function of Ct using the observed binary AT outcomes and (2) compute expected sensitivity by averaging the fitted PPA over supplier A's Ct values via equation 1.

The described viral load balance processes removed the effect of the Ct distribution on sensitivity, providing a common base for comparison and evaluation of the test performance.

Table 1 presents a glossary of terms and their corresponding meanings.

Table 1. Glossary of relevant terms and corresponding meanings.

Term	Definition			
Antigen test (AT)	Lateral flow antigen test			
Target	Specific analyte that the test is designed to detect (protein present in a biological matrix sample)			
Cycle threshold (Ct)	qRT-PCRa cycle at which the fluorescence signal crosses a set threshold above background			
Target concentration	It is the concentration of the target protein, expressed by cycle thresholds or $ng\ mL^{-1}$, or by plaque forming units of virus mL^{-1}			
Target concentration distribution	The distribution of target concentrations among the tested population; when grouped into concentration ranges, it can be represented as a histogram.			
Sensitivity	Proportion of positive cases detected by the antigen tests according to the reference qRT-PCR gold standard. It represents the percent positive agreement.			
Percent positive agreement (PPA)	In a Bernoulli process, it is the probability that the test outcome is positive; in the context of antigen tests, this probability varies with the target concentration.			
Percent positive agreement function (PPAf)	It is a function assigning the value of the probability of positive agreement for a given target concentration.			
Distribution-balanced sensitivity	The modeled value of the sensitivity at a selected (balanced) cycle distribution distribution different from that of the real-world dataset.			
Reference distribution	A distribution of the target concentration that is adopted as reference to model the sensitivity.			

 ${}^a\mbox{qRT-PCR:}$ quantitative reverse transcription polymerase chain reaction.

Results

Raw Positive Agreement Statistics

This section describes the basic performance statistics of the ATs of the 4 suppliers analyzed, and the estimated PPAfs, based on the binary data collected from the Chelsea study

[15]. The agreement matrix was determined for each supplier AT, and the common performance agreement fractions were calculated: sensitivity, specificity, positive prediction, negative prediction, and total prediction. Table 2 displays the basic performance statistics for each one of the test suppliers, including the Clopper-Pearson 95% confidence limits [16].

Table 2. Basic performance statistics for COVID-19 in vitro diagnostics suppliers A, B, C, and D.

Supplier	Positive agreement cases, n	Total cases, n	Value	Lower 95% confidence limit	Upper 95% confidence limit
A					
Sensitivity	177	211	0.84	0.78	0.89
Specificity	55	57	0.96	0.88	1.00
Positive prediction	177	179	0.99	0.96	1.00
Negative prediction	55	89	0.62	0.51	0.71
Total agreement	232	268	0.87	0.82	0.90
В					
Sensitivity	117	156	0.75	0.67	0.82
Specificity	90	91	0.99	0.94	1.00
Positive prediction	177	118	0.99	0.95	1.00
Negative prediction	90	129	0.70	0.61	0.77
Total agreement	207	247	0.84	0.79	0.88
C					
Sensitivity	55	85	0.65	0.54	0.75
Specificity	144	144	1.00	0.97	1.00
Positive prediction	55	55	1.00	0.94	1.00
Negative prediction	144	174	0.83	0.76	0.88
Total agreement	199	229	0.87	0.82	0.91
D					
Sensitivity	35	43	0.81	0.67	0.92
Specificity	107	114	0.94	0.88	0.97
Positive prediction	35	42	0.83	0.69	0.93
Negative prediction	107	115	0.93	0.85	0.97
Total agreement	142	157	0.90	0.88	0.95

Sensitivities show large differences across the suppliers A, B, C, and D, with values 0.84, 0.75, 0.65, and 0.81, respectively. A comparison plot of the raw AT sensitivities for each supplier and confidence limits is shown (Figure 1). Differences are significant with a large departure of 19% (percentage points of the sensitivity) between suppliers A

and C. However, the histograms of qRT-PCR Cts supporting the sensitivity calculations have marked differences across the suppliers (Figure 2). Note that suppliers A and D have a larger proportion of low Cts (large viral sample concentration). On the other hand, supplier C has a larger representation of large Cts (low viral sample concentration).

Figure 1. Raw sensitivities resulting from the real-world Chelsea study for lateral flow in vitro diagnostics suppliers A, B, C, and D. The boxes and whiskers indicate the median and 50% and 95% confidence limits calculated using the Clopper-Pearson statistical method. The horizontal dotted line across all histograms indicates the 0.8 sensitivity value, which is acceptable for in vitro diagnostics clinical performance according to regulatory standards at 0.8 sensitivity for COVID-19 antigen tests.

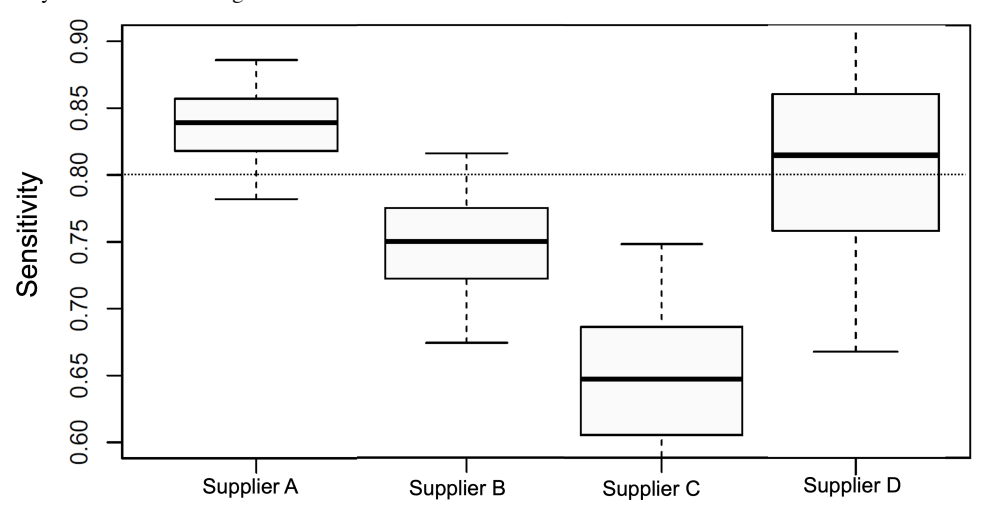
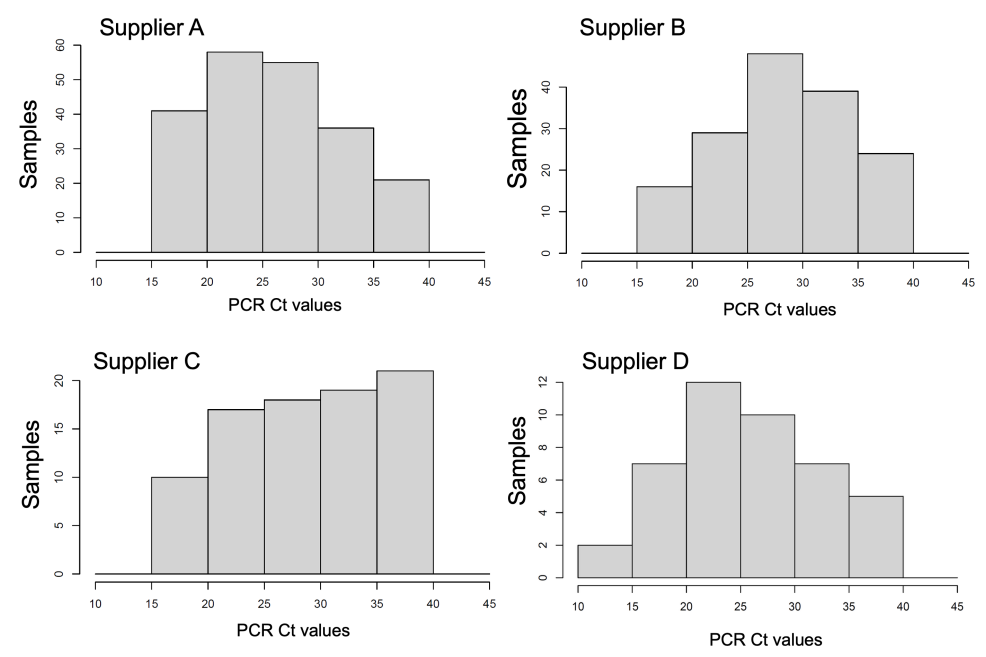


Figure 2. Histogram distributions of cycle thresholds (Cts) for antigen test suppliers A-D using quantitative reverse transcription polymerase chain reaction (qRT-PCR) Cts for each antigen test supplier's dataset. Cts are the average of N and ORFab gene segments of SARS-CoV-2 and reported from Clinical Laboratory Improvement Amendments–certified laboratory using a PerkinElmer SARS-CoV-2 Food and Drug Administration–approved kit.

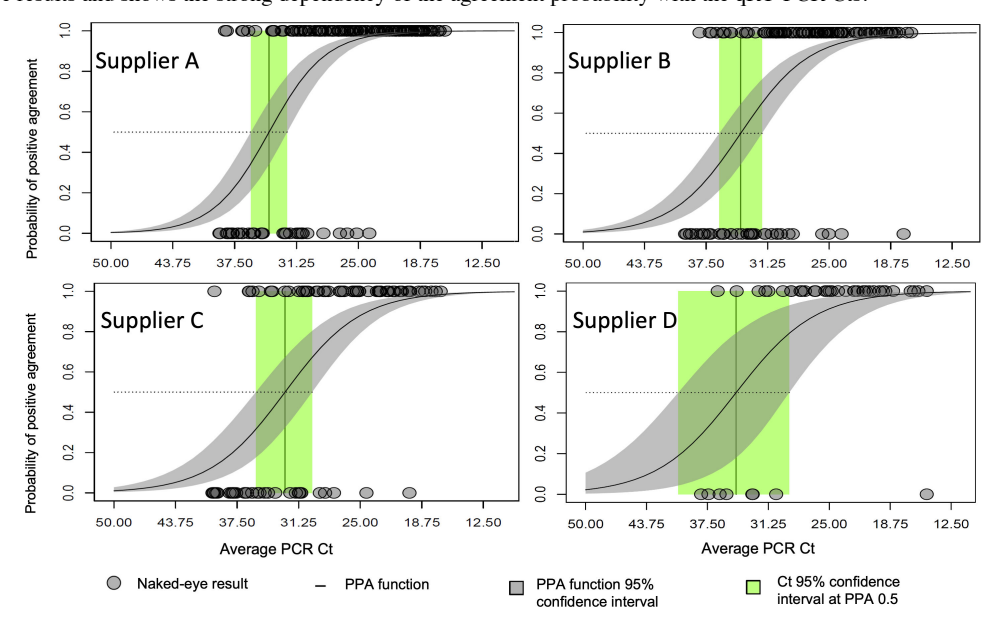


Probability of Positive Agreement Functions

Raw sensitivities (Figure 1) superpose the effects of the viral concentration support to the true performance of the ATs. Following our method, a first step to decouple the 2 effects is estimating the PPAf from the raw data of each AT supplier by logistic regression, as explained in the previous section.

Figure 3 shows the binary data collected for each AT supplier plotted against the Cts and the estimated PPAf for each test supplier. The estimation of the PPAf by fitting the observed binary AT data also provides the description of the uncertainties in the PPAf. With the 95% confidence intervals of the PPAf, our formulation estimates the full distribution of the PPA conditioned to the Ct value.

Figure 3. Positive percent agreement (PPA) as a function of the quantitative reverse transcription polymerase chain reaction (qRT-PCR) cycle thresholds (Cts) for naked-eye assessments of the Chelsea project participants after self-application of the antigen tests. Naked-eye assessments of the antigen test result are plotted in the vertical axis with value 1 for positive and 0 for negative. The PPA function is obtained by logistic regression of the binary naked-eye results and shows the strong dependency of the agreement probability with the qRT-PCR Cts.



The PPAfs for suppliers A and B are similar (Figure 3). Note that the Ct of median probability (ie, limit of detection at probability P=.50) and the slope of the line function are

similar to one another. The PPAf for supplier C shows a slightly larger Ct at median probability and lower slope of the function. The PPAf for supplier D is also close to the A

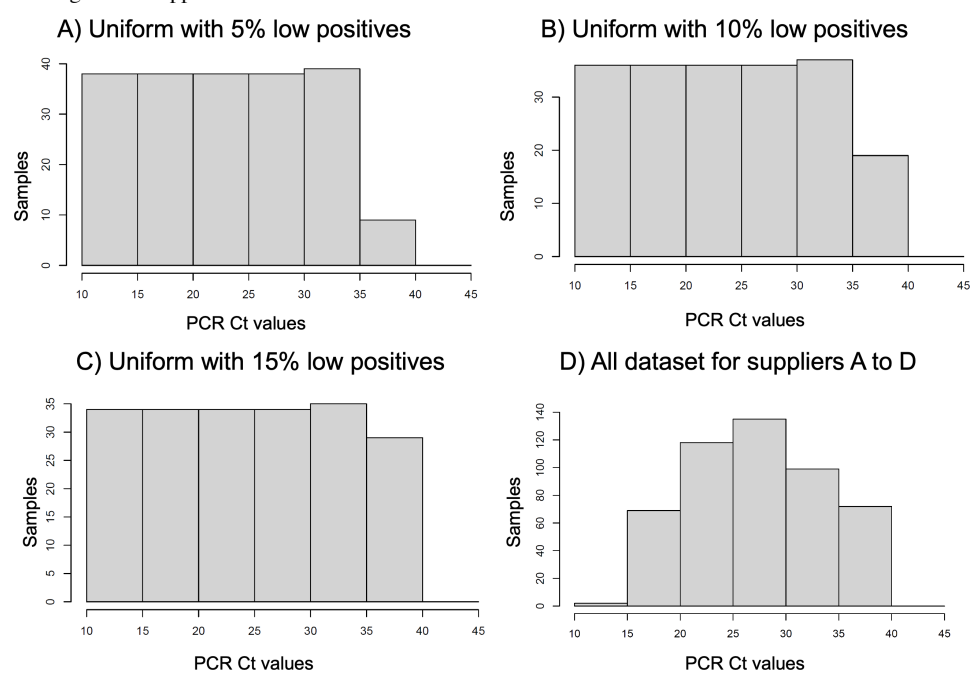
and B functions but shows a wider range of uncertainties, also expected from the smaller dataset supporting supplier D.

Several factors influence the estimation of the PPAf: the representation of the Ct range, the balance between positive and negative samples, and the overall sample size. Smaller sample sizes increase the uncertainty of the PPAf, as illustrated in the case of supplier D. However, in this case, the estimation remained reliable because the Ct range and the positive-negative representation were sufficiently well balanced. The Ct values in supplier D's dataset are comparable to those observed in other supplier datasets. Similarly, the distribution of positive and negative samples is appropriate, with a higher frequency of negatives at lower viral loads (ie, higher Ct values), as expected. In contrast, datasets with limited coverage of the Ct range, underrepresentation of positives or negatives, or a distribution that fails to reflect the expected polarization, with negatives concentrated at higher Ct values and positives at lower Ct values, would not support a reliable estimation.

Reference Distributions of Viral Load

Due to the specific Ct value distributions, the comparison of raw sensitivities is biased by the uneven distribution of the Ct support. This is shown by the corresponding histograms (Figure 2). Utilizing the balance methodology, we computed the sensitivities of the ATs from the 4 suppliers across 4 distinct reference distributions of the Cts. The sample statistics of the PPA exhibit particular sensitivity to low positive samples, that is, those with low viral concentration. Consequently, we opt for a uniform distribution of qRT-PCR cycles spanning 10-35 Cts, with variable proportions within the 35-40 range, to underscore the significance of representing low-positive cases in the overall sample PPA (Figure 4A-C). Additionally, we employed the combined Ct distribution of all 4 tests as a reference, that is, the joint positive qRT-PCR Ct counts of the 4 suppliers' data (Figure 4D).

Figure 4. Comparison of selected reference distributions of the raw data. Histograms A, B, and C correspond to 200 dataset points with a range of low virus load (from 5% to 15% of sample at 35-40 quantitative reverse transcription polymerase chain reaction [qRT-PCR] cycle threshold [Ct] range) and uniform distribution in the range of high-to-moderate virus load (10-35 qRT-PCR Ct range). Histogram D corresponds to the overlap of the 4 antigen test in vitro diagnostics suppliers' real-world data.



We present 4 different Ct distributions to illustrate how Ct values, and therefore virus load, influence the adjusted sensitivity. The purpose of the distribution-balancing process is 2-fold: (1) to enable accurate comparison of AT sensitivities across studies and (2) to improve real-world sensitivity estimation. First, comparing sensitivities across studies becomes more reliable when distribution-balanced is referenced to a common distribution. Second, clinical studies often have limited numbers of cases and may not adequately reflect the real-world distribution of target concentrations observed in broader populations (eg, regional or national data). In this context, distribution-balanced sensitivity provides a closer approximation of real-world performance. For our clinical dataset, the distribution that best

represents the broader population is the overall Ct dataset (Figure 4D), as it includes all cases pooled from the 4 devices.

Sensitivities for the Reference Distributions

According to the described viral load balance method, we estimated the sensitivities of the ATs of the 4 suppliers (Figure 5) over each one of the reference distributions (Figure 4) utilizing the PPAf. It is interesting to compare the results shown (Figure 4) to the raw sensitivities previously calculated (Figure 1). Although the order of performance of the 4 suppliers has been preserved, in order of best to worst

performances, the order was supplier A, B, D, and C. The sensitivity differences are smaller among suppliers once the effect of the source distribution is removed. The difference between suppliers A and C is only at 5% instead of the 19% for the raw sensitivity calculation. A large proportion of the

raw sensitivity difference between these 2 suppliers originated from the overrepresentation of high viral concentration samples for supplier A and the overrepresentation of low viral concentration samples for supplier C.

Figure 5. Sensitivities of antigen test brands calculated from reference distributions of cycle thresholds as shown in Figure 4. The boxes and whiskers indicate median and 50% and 95% confidence limits. Horizontal dotted line across each panel shows the threshold of 0.8 sensitivity acceptable for in vitro diagnostics clinical performance according to regulatory standards for COVID-19 antigen tests. RW: real world.

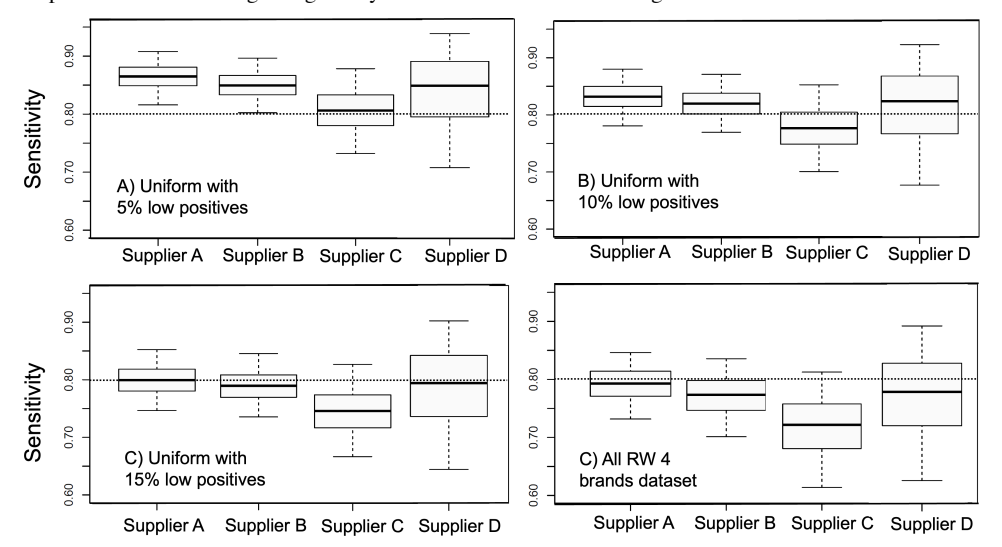


Figure 5 shows the impact of the reference distributions of Ct values on the resulting sensitivity. The absolute value of the sensitivity shows a variation of over 8% difference across the different distributions-larger than the difference across the supplier sensitivities. In particular, the fraction of low virus concentration positives plays an important role, as expected: the PPAfs (Figure 3) show that the probability of positive agreement is very low for low positives (35-40 Cts) in all suppliers. The indicated line at 0.8 sensitivity in Figure 5 helps to illustrate this point. With the reference distribution including 5% of low positives, the 4 suppliers have sensitivities over the 0.8 threshold. With the reference distribution including 15% of low positives, suppliers B and C are below the threshold, whereas suppliers A and D are borderline at the 0.8 threshold value. With the distribution that combines the 4 suppliers' observed samples, all the suppliers are below the 0.8 threshold.

Discussion

Accurate estimation of AT performance in real-world studies is often confounded by heterogeneous viral load distributions, sample collection conditions, and demographic factors [17]. In particular, the Ct values derived from qRT-PCR, which serve as a surrogate for viral concentration, exhibit considerable variability across study populations. This variability can bias sensitivity—or PPA—estimates when derived directly from unbalanced datasets.

To address the limitation, we introduce a mathematically grounded approach that estimates a PPAf via logistic regression and then recalculates sensitivity over a standardized reference Ct distribution. This method transforms

raw sensitivity estimates into a harmonized metric that is independent of the original data's viral load distribution, enhancing comparability across studies and diagnostic platforms. By modeling the entire range of Ct values, rather than focusing solely on predefined low-positive bins, our approach enables more comprehensive and statistically balanced evaluations. A reference distribution of qRT-PCR Ct values serves as a standardized representation of viral load across a target population, enabling consistent evaluation of diagnostic test sensitivity. Unlike raw distributions derived from individual clinical studies-which are subject to variability in recruitment timing, population demographics, testing strategies, and local epidemiology-a reference distribution is designed to reflect a controlled or representative viral load profile against which diagnostic performance can be compared. The reference Ct distribution may be empirically derived from large, well-characterized datasets collected during peak transmission periods or constructed synthetically based on known viral kinetics in the population. For example, an ideal reference might be a unimodal distribution centered around the Ct range associated with peak transmissibility and highest clinical relevance (eg, Ct 20-30), or it might reflect the full spectrum of observed viral loads (eg, Ct 10-40), weighted to mirror realistic clinical case presentations across settings. The purpose of applying such a reference is to enable adjusted sensitivity calculations that are independent of the viral load biases inherent in the original data. This is particularly important when comparing AT performance across different suppliers or studies, where raw sensitivities may differ simply due to the proportion of high- or low-Ct samples in each dataset. In the diagnostic settings, a broader distribution capturing both early and late stages of infection may be more appropriate. Ultimately, the

choice of reference distribution must be consistent, allowing for harmonized sensitivity comparisons that reflect diagnostic utility across diverse real-world scenarios.

While regulatory frameworks have moved toward including "lower viral load specimens" in performance assessments to mitigate overestimation, these approaches often lack generalizability and do not account for the full spectrum of observed Ct values. Our methodology advances this paradigm by providing a distribution-based recalibration mechanism, capturing the full continuum of viral concentrations, and generating sensitivity estimates that are both internally consistent and externally comparable. Critically, FDA Emergency Use Authorization evaluation criteria anchored to qRT-PCR (including use of highly sensitive PCR comparators and mandated proportions of "low-positive" samples) shaped apparent clinical sensitivity and reinforced PCR-first policies for confirmation, whichdespite PCR's analytical advantages-dampened uptake of antigen testing for rapid, frequent screening where time-toresult drives transmission control.

Furthermore, genetic strain diversity, specific amino acid mutations in the SARS-CoV-2 nucleoprotein, and host disease–related comorbidities and immunological factors [18,19] may influence AT performance. These factors that could alter antigen detection are also limitations that apply to molecular diagnostics, where ongoing monitoring of performance and vigilance for unexpected results are required. To date, both the original SARS-CoV-2 Delta strain

and its descendant Omicron lineages have been detected with comparable efficiency across ATs. From the list of virus lineages we reported, we did not detect differences in AT performance. Kinetics of binding or other more sensitive analysis was outside the scope of this paper. Under the assumption of a relatively genetically uniform circulating viral strain, PCR Ct-based adjustments provided a pragmatic and scientifically valid strategy to reduce bias in estimating AT performance. In contexts where variant heterogeneity becomes relevant, the proposed distribution balancing approach could be extended by calculating variant-specific PPAfs and integrating them into proportionally weighted models. While Ct values serve as quantitative proxies with platform-dependent variability, internal laboratory calibrations (ie, processing of all nasal swabs within the same laboratory and RNA extraction and PCR protocol) mitigate this source of error. In the study, a single RNA extraction and PCR protocol of the Clinical Laboratory Improvement Amendment generated Ct values, thereby minimizing variability and controlling for recalibration effects.

In summary, we propose a robust statistical framework that corrects for real-world sampling biases through distributional modeling. This approach yields adjusted sensitivity estimates that more accurately reflect intrinsic test performance, thereby supporting improved diagnostic evaluation, regulatory decision-making, and public health comparisons across populations and settings.

Acknowledgments

We thank the sponsors of the work, the Reagan-Udall Foundation for the Food and Drug Administration, and the program Rapid Acceleration of Diagnostics for Underserved Populations (RADx-UP) Coordination and Data Collection Center of the National Institutes of Health, to the Broad Institute for processing and reporting the polymerase chain reaction (PCR)—positive COVID-19 cases and for executing the viral genome sequencing. We would also like to thank Adriana Mendoza for the coordination of the studies; Dr Karen Weeks and Anna Roberts of Eco Laboratory, Acton, MA, for PCR processing of the samples; Dr Lee Gehrke for advice and virology expertise; and Dr Alfred Harding for virus isolation for PCR calibrations. We also acknowledge CorDx for providing antigen tests and the Chelsea Housing Authority for offering guidance and support for the study. We also thank all the participants of the study for their valuable contribution and attendance.

The research was supported by the Reagan-Udall Foundation through grant 02282022 RUF and by the Duke University National Institutes of Health RADx-UP program (grant R0502A) to IDx20 Inc and a RADx-UP CDCC award (1U24MD016258-01) and subaward (303002431), and The Broad Institute SARS-CoV-2 award 75D30122C15113 from the Centers for Disease Control and Prevention.

Data Availability

The data are publicly available at ClinicalTrials.gov (NCT05884515) and upon request at the RADx-UP website for CorDx data. A public access web tool to calculate the percent positive agreement function as well as to execute the distribution-balanced sensitivity methodology is available at [20].

Authors' Contributions

Conceptualization: IB (lead), MB (equal), SH (secondary)

Data curation: AM, DG, DH, IB, JA, MB, RC

Formal analysis: DG (supporting), JA (supporting), LR (supporting), MB (lead), NS (supporting)

Funding acquisition: IB

Investigation: DG, IB, LR, MB, NS, SH

Methodology: IB, MB

Project administration: DH (supporting), IB (lead)

Resources: IB

Supervision: IB, DH, MB, SH

Validation: AM, DG, LR, NS, RC

Writing – original draft: IB (supporting), MB (lead) Writing – review & editing: IB (lead), MB (supporting)

Conflicts of Interest

IB is a founder of IDX20, a company affiliated with this study. MB is a founder of Info Analytics Innovations, a company also affiliated with this study. The authors declare no additional conflicts of interest.

References

- 1. Tillmann HL. Hepatitis C virus core antigen testing: role in diagnosis, disease monitoring and treatment. World J Gastroenterol. Jun 14, 2014;20(22):6701-6706. [doi: 10.3748/wjg.v20.i22.6701] [Medline: 24944462]
- 2. Chartrand C, Tremblay N, Renaud C, Papenburg J. Diagnostic accuracy of rapid antigen detection tests for respiratory syncytial virus infection: systematic review and meta-analysis. J Clin Microbiol. Dec 2015;53(12):3738-3749. [doi: 10.1128/JCM.01816-15]
- 3. Ty Hang V, Minh Nguyet N, The Trung D, et al. Diagnostic accuracy of NS1 ELISA and lateral flow rapid tests for dengue sensitivity, specificity and relationship to viraemia and antibody responses. PLoS Negl Trop Dis. 2009;3(1):e360. [doi: 10.1371/journal.pntd.0000360]
- 4. Lawn SD, Dheda K, Kerkhoff AD, et al. Determine TB-LAM lateral flow urine antigen assay for HIV-associated tuberculosis: recommendations on the design and reporting of clinical studies. BMC Infect Dis. Dec 2013;13(1):407. [doi: 10.1186/1471-2334-13-407]
- 5. Augustine R, Das S, Hasan A, et al. Rapid antibody-based COVID-19 mass surveillance: relevance, challenges, and prospects in a pandemic and post-pandemic world. J Clin Med. Oct 21, 2020;9(10):3372. [doi: 10.3390/jcm9103372] [Medline: 33096742]
- 6. Peto T, Affron D, Afrough B, et al. COVID-19: rapid antigen detection for SARS-CoV-2 by lateral flow assay: a national systematic evaluation of sensitivity and specificity for mass-testing. EClinicalMedicine. Jun 2021;36:100924. [doi: 10.1016/j.eclinm.2021.100924]
- 7. Pickering S, Batra R, Merrick B, et al. Comparative performance of SARS-CoV-2 lateral flow antigen tests and association with detection of infectious virus in clinical specimens: a single-centre laboratory evaluation study. Lancet Microbe. Sep 2021;2(9):e461-e471. [doi: 10.1016/S2666-5247(21)00143-9] [Medline: 34226893]
- 8. Pollock NR, Jacobs JR, Tran K, et al. Performance and implementation evaluation of the Abbott BinaxNOW rapid antigen test in a high-throughput drive-through community testing site in Massachusetts. J Clin Microbiol. Apr 20, 2021;59(5):1-10. [doi: 10.1128/JCM.00083-21] [Medline: 33622768]
- 9. Wagenhäuser I, Knies K, Rauschenberger V, et al. Clinical performance evaluation of SARS-CoV-2 rapid antigen testing in point of care usage in comparison to RT-qPCR. EBioMedicine. Jul 2021;69:103455. [doi: 10.1016/j.ebiom.2021. 103455] [Medline: 34186490]
- 10. Singanayagam A, Patel M, Charlett A, et al. Duration of infectiousness and correlation with RT-PCR cycle threshold values in cases of COVID-19, England, January to May 2020. Euro Surveill. Aug 2020;25(32):2001483. [doi: 10.2807/1560-7917.ES.2020.25.32.2001483] [Medline: 32794447]
- 11. Rabaan AA, Tirupathi R, Sule AA, et al. Viral dynamics and real-time RT-PCR Ct values correlation with disease severity in COVID-19. Diagnostics (Basel). Jun 15, 2021;11(6):1091. [doi: 10.3390/diagnostics11061091] [Medline: 34203738]
- 12. Fox MP, Lash TL, Bodnar LM. Common misconceptions about validation studies. Int J Epidemiol. Aug 1, 2020;49(4):1392-1396. [doi: 10.1093/ije/dyaa090] [Medline: 32617564]
- 13. Walker SH, Duncan DB. Estimation of the probability of an event as a function of several independent variables. Biometrika. Jun 1967;54(1):167-179. [doi: 10.2307/2333860] [Medline: 6049533]
- 14. Corman VM, Haage VC, Bleicker T, et al. Comparison of seven commercial SARS-CoV-2 rapid point-of-care antigen tests: a single-centre laboratory evaluation study. Lancet Microbe. Jul 2021;2(7):e311-e319. [doi: 10.1016/S2666-5247(21)00056-2] [Medline: 33846704]
- 15. Community study to evaluate the performance of COVID-19 frequent antigen testing at home through digital health reporting. Reagan-Udall Foundation. 2022. URL: https://reaganudall.org/clinical-trial/evaluation-home-use-covid-19-frequent-antigen-testing-and-data-reporting [Accessed 2025-10-09]
- 16. Clopper CJ, Pearson ES. The use of confidence or fiducial limits illustrated in the case of the binomial. Biometrika. 1934;26(4):404-413. [doi: 10.1093/biomet/26.4.404]
- 17. Practical applications of real-world evidence to enable regulatory submissions. Reagan-Udall Foundation. URL: https://reaganudall.org/sites/default/files/2023-09/PIVD%20Commentary%20FINAL3419899_%20bf%20092123.pdf [Accessed 2025-10-10]

- 18. Song Q, Bates B, Shao YR, et al. Risk and outcome of breakthrough COVID-19 infections in vaccinated patients with cancer: real-world evidence from the National COVID Cohort Collaborative. J Clin Oncol. May 1, 2022;40(13):1414-1427. [doi: 10.1200/JCO.21.02419] [Medline: 35286152]
- 19. Del Vecchio C, Cracknell Daniels B, Brancaccio G, et al. Impact of antigen test target failure and testing strategies on the transmission of SARS-CoV-2 variants. Nat Commun. Oct 5, 2022;13(1):5870. [doi: 10.1038/s41467-022-33460-0] [Medline: 36198689]
- 20. IDX20. URL: https://www.idx20.us/ [Accessed 2025]1010

Abbreviations

AT: antigen test Ct: cycle threshold

IRB: institutional review board **PDF:** probability density function **PPA:** percent positive agreement

PPAf: percent positive agreement function

qRT-PCR: quantitative reverse transcription polymerase chain reaction

Edited by Sean Hacking; peer-reviewed by Ali Ahsan, Carol Cheung, Qianqian Song; submitted 08.Nov.2024; final revised version received 26.Aug.2025; accepted 13.Sep.2025; published 20.Oct.2025

Please cite as:

Bosch M, Moreno A, Colmenares R, Arocha J, Hoche S, Garcia A, Hall D, Garcia D, Rudtner L, Salcedo N, Bosch I Estimating Antigen Test Sensitivity via Target Distribution Balancing: Development and Validation Study JMIR Bioinform Biotech2025;6:e68476

URL: https://bioinform.jmir.org/2025/1/e68476

doi: 10.2196/68476

© Miguel Bosch, Adriana Moreno, Raul Colmenares, Jose Arocha, Sina Hoche, Auris Garcia, Daniela Hall, Dawlyn Garcia, Lindsey Rudtner, Nol Salcedo, Irene Bosch. Originally published in JMIR Bioinformatics and Biotechnology (https://bioinform.jmir.org), 20.Oct.2025. This is an open-access article distributed under the terms of the Creative Commons Attribution License (https://creativecommons.org/licenses/by/4.0/), which permits unrestricted use, distribution, and reproduction in any medium, provided the original work, first published in JMIR Bioinformatics and Biotechnology, is properly cited. The complete bibliographic information, a link to the original publication on https://bioinform.jmir.org/, as well as this copyright and license information must be included.